

# Simultaneous surface acoustic wave and surface plasmon resonance measurements: electrodeposition and biological interactions monitoring

J.-M Friedt,\* L. Francis, G. Reekmans, R. De Palma, and A. Campitelli†

*IMEC, MCP/BIO, Kapeldreef 75, 3001 Leuven, Belgium*

U.B. Sleytr

*Center for Ultrastructure Research and Ludwig Boltzmann Institute*

*for Molecular Nanotechnology, Universität für Bodenkultur Wien,*

*Gregor-Mendel-Str. 33, A-1180 Vienna, Austria*

(Dated: February 7, 2020)

## Abstract

We present results from an instrument combining surface acoustic wave (SAW) propagation and surface plasmon resonance (SPR) measurements. The objective is to use two independent methods, the former based on adsorbed mass change measurements and the latter on surface dielectric properties variations, to identify physical properties of protein layers, and more specifically their water content. We display mass sensitivity calibration curves using electrodeposition of copper leading to a sensitivity in liquid of  $150 \pm 15 \text{ cm}^2/\text{g}$  for the Love mode device used here, and the application to monitoring biological processes. The extraction of protein layer thickness and protein to water content ratio is also presented for S-layer proteins under investigation. We obtain respectively  $4.7 \pm 0.7 \text{ nm}$  and  $75 \pm 15\%$ .

PACS numbers: 68.47.Pe

---

\*Electronic address: friedtj@imec.be

†Electronic address: campi@imec.be

## I. INTRODUCTION

Surface plasmon resonance (SPR) is a well accepted direct detection technique for monitoring biological processes [1, 2]. While ellipsometry is another well known method for analyzing thin film properties [3], its use in liquid medium for monitoring biochemical reactions is made difficult by the varying environment through which the probing light beam has to propagate. In the Kretschmann configuration, the laser generating the SPR evanescent wave is only propagating through the substrate, leading to a better control over the influence of the various buffer solutions used during a protein adsorption experiment.

The use of various acoustic wave devices for monitoring bound mass changes in liquid media is well known [4]. Love mode devices, based on the propagation of a guided shear acoustic wave, present sensitivity improvements over the more usual quartz crystal microbalance [5] as well as a compatibility with measurements in liquids.

We take advantage of the unique geometrical setup of the surface acoustic wave (SAW) device which leaves the backside of the quartz wafer free of electrodes to inject a laser in order to generate an evanescent surface plasmon on the gold coated sensing area. Such a setup enables simultaneous estimates of the bound mass and dielectric surface properties changes during electrochemical and biochemical reactions occurring on the sensing electrode [6, 7].

Estimates of water content in protein layers is an important topic in the development of biosensors, since the detection sensitivity is directly related to the number of active sites on the surface of the sensor to which the receptor molecules are bound. When physical measurements of this bound layer are performed, such as via SPR or acoustic measurements, a large water content will lead to overestimates of the potential detection limit of the biosensor due to an overestimate of number of molecules bound to the surface. From a more fundamental point of view, determining water level content should provide more accurate physical parameters of the protein layer itself such as density and optical index by allowing the subtraction of the influence of water once it has been identified.

## II. EXPERIMENTAL DATA

We use a modified commercial SPR instrument (IBIS II, IBIS Technologies BV, The Netherlands) to detect the surface plasmon resonance angle after replacing the gold coated glass slide by a Love mode SAW device (Fig. 1). The excitation laser in this instrument has a wavelength of 670 nm. All reflected intensity *vs.* angle curves (6 ° angle span recorded on a 200 pixels CCD array) were recorded and later fitted by a polynomial to extract with high accuracy the position of the dip. The acoustic wave device is made of a 500  $\mu\text{m}$  thick ST-cut quartz wafer on which 200 nm thick sputtered *Al* interdigitated electrodes are patterned. The surface is coated by a 1.13  $\mu\text{m}$  PECVD silicon dioxide layer acting as a guiding layer, and the 4.9 $\times$ 5.4 mm<sup>2</sup> sensing area is coated with 10 nm *Ti* and 50 nm *Au*. This area acts both as a working electrode for electrochemistry or a grounded electrode during biochemical experiments, as well as a supporting layer for the surface plasmon resonance generation. The influence of the SAW device substrate over the detection of the SPR is limited to interference patterns due to the birefringence of the quartz, and the optical index mismatch between the quartz and the deposited silicon dioxide layer. The former effect is reduced by orienting the optical axis of quartz so that it is in the plane defined by the normal to the sensing surface and the wavevector of the laser, thus minimizing the optical index difference between the ordinary and the extraordinary axis. The remaining interference patterns lead to fringes with a low enough contrast that the surface plasmon peak is easily identified and tracked during the experiments.

The phase of the SAW delay line is monitored at a fixed frequency using a network analyzer HP4396A at 123.200 MHz. The phase shift is converted to a frequency shift thanks to the linear phase to frequency relationship recorded in the Bode plot. The observed phase shift leads to a frequency shift (as would be observed in a phase locked loop configuration) which in turn can be converted to an adsorbed mass change through the sensitivity of the device.

We first electrodeposited copper on the surface in order to calibrate the mass sensitivity of the acoustic wave device in liquid medium (Fig. 2) [8]. At the same time, the SPR displayed resonance angle shifts due to the varying potential [9]. When the voltage applied by the potentiostat is above 0.2 V with respect to the *Cu* pseudo reference electrode, the SPR angle slightly shifts due to the electroreflectance effect described by Kötzt *et al.* [9].

Below 0.2 V, under potential deposition starts depositing a mono layer of *Cu* atoms on the *Au* surface as visible both in the phase shift of the SAW device and as a reversal of the trend of the angle shift of the SPR. Below 0 V, a rough *Cu* layer is deposited, leading to a loss of the SPR peak and a large phase shift of the SAW device due to the large added mass. The rough, discontinuous film of copper clusters a few tens to hundreds of nanometers high was observed by in-situ AFM imaging (data not shown [8]). Simulating the influence of sub-wavelength metallic structures on the surface plasmon resonance is a difficult task [10, 11] which we have not attempted to solve. Simultaneously, the SAW device displays a frequency drop  $\Delta f$  due to the added mass  $\Delta m$  to the sensing electrode, leading with the combination of the current measurement from the potentiostat to a direct estimate of the mass sensitivity  $S = \frac{\Delta f}{f_0} \frac{A}{\Delta m}$  where  $A = 0.49 \times 0.54 \text{ cm}^2$  is the area of the sensing working electrode and  $f_0 = 123.200 \text{ MHz}$  the base frequency of the SAW device. The electrodeposited mass is deduced from the current measurement  $I$  with a sampling period  $\delta t$ :  $\Delta m = \frac{\sum_j I_j \times \delta t}{F} \times \frac{M}{n_e}$  where  $F = 96485 \text{ C}$  is the Faraday constant,  $M$  the molar weight of the electrodeposited metal and  $n_e$  the number of electrons exchanged for each metallic atom reduced. The resulting sensitivity for the Love mode device under consideration here is  $150 \pm 15 \text{ cm}^2/\text{g}$ .

Once the mass sensitivity of the SAW is calibrated, we adsorbed on the same device a crystalline monolayer of S-layer proteins (100  $\mu\text{g}/\text{ml}$  of the protein SbpA of *Bacillus sphaericus* CCM 2177 in 0.5 mM tris, 10 mM *CaCl*<sub>2</sub>, pH=9 buffer) [12, 13] while monitoring simultaneously with the SAW device the mass variation and with SPR the surface dielectric change. The adsorption and desorption steps, the latter being possible with the use of 2 % *NaOCl*, was repeated several times (Fig. 3). A property of this protein which makes it suitable for calibration of a new instrument is that it only forms a monolayer and will not stack to multiple layers even at high concentrations.

### III. DISCUSSION

The parameters required for analyzing the SAW data are the layer thickness  $d$  and the layer density  $\rho_{layer}$ . The parameters required for analyzing the SPR data are the common layer thickness  $d$  and the optical index  $n$  of the adsorbed layer. We thus have three free parameters and only two measurements, namely the adsorbed mass per unit area and an SPR

resonance angle shift which is a function of both  $n$  and  $d$ . The two options are to add one more measurement parameter, such as an SPR dip position as a function of wavelength which would lead to a unique identification of  $d$  and  $n$  [14], or to reduce the number of variables by adding the assumption that the layer is made of a homogeneous mixture of a proportion  $x$  of protein and  $1 - x$  of water. The layer density  $\rho_{layer}$  is then  $\rho_{layer} = x\rho_{protein} + (1 - x)\rho_{water}$  where  $\rho_{protein}$  is assumed to be equal in the 1.2 g/cm<sup>3</sup> to 1.4 g/cm<sup>3</sup> range [3, 15, 16, 17] and  $\rho_{water} = 1$  g/cm<sup>3</sup> is the density of water. Similarly, we use then the optical index of the layer  $n_{layer} = xn_{protein} + (1 - x)n_{water}$  with the optical index of the protein layer assumed to be in the  $n_{protein} = 1.45$  to 1.465 range [1, 16, 17] and that of water  $n_{water} = 1.33$ . The remaining unknown parameters are then the layer thickness  $d$  and the water content proportion  $1 - x$ . By simulating a stack of planar multilayers (glass  $n_{glass} = 1.518$ , 1200 nm silicon dioxide  $n_{SiO_2} = 1.45$ , 2 nm titanium  $n_{Ti} = 2.76 + i3.84$  [18], 50 nm gold  $n_{Au} = 0.14 + i3.697$  [18], proteins, water) for the angle shift as a function of water content and layer thickness, one obtains a set of pairs of values for these two parameters compatible with the observed angle shift (Fig. 4, bottom). Then, by calculating the mass per unit area  $\Delta m = \rho d$ , a comparison with the experimentally observed adsorbed mass as seen from the phase shift of the SAW device leads to a unique set of parameters both compatible with the optical index change and the adsorbed mass (Fig. 4, top). In the case under consideration here, an observed angle shift of 380 to 400 m<sup>o</sup> and an adsorbed mass of 540 to 580 ng/cm<sup>2</sup> is only compatible with  $x = 0.75 \pm 0.15$  and  $d = 4.7 \pm 0.7$  nm. The thickness result is compatible with atomic force microscope (AFM) measurements in liquid [13] while the mass per unit area is compatible with morphological data obtained by electronic microscopy [12]. While the main source of uncertainty is due to the wide possible values of the density and optical index reported in the literature, the experimental results display good reproducibility. The water content is lower than that observed by other authors for different kinds of proteins [3, 17] but compatible with the 30 to 78% value cited in Ref. [19]. The dense packing of protein is explained by the regular arrangement of identical S-layer subunits in the p4 lattice [20, 21].

#### IV. CONCLUSION

We have shown here how the combination of Love mode SAW device with SPR provides advantageous combinations of information on the bound mass as well as on the dielectric

changes when monitoring protein adsorption. The resulting protein layer thickness and protein content percentage, respectively  $d = 4.7 \pm 0.7$  nm and  $x = 75 \pm 15$  %, is in agreement with independent AFM estimates.

## V. ACKNOWLEDGMENTS

The SAW transducers were fabricated within the framework of a Belgian PhD scholarship program (Fonds pour la formation à la Recherche dans l'Industrie et dans l'Agriculture – FRIA). We wish to thank R. Giust (LOPMD, Besançon, France) for kindly providing SPR simulation routines.

FIG. 1: Experimental setup including, from bottom to top: the cylindrical glass prism for injecting the laser, the quartz wafer patterned with interdigital transducers for generating the acoustic waves and coated with a thin ( $1.2 \mu\text{m}$ )  $\text{SiO}_2$  layer, and the SU8 walls supporting the glass slides capping preventing the contact of the liquid over the transducers area. We indicate for clarity on the top graph the equivalent frequency shift (in kHz) and on the bottom graph the equivalent mass and calculated sensitivity.

FIG. 2: SAW sensitivity calibration curves using copper electrodeposition. From bottom to top: potentiostat current and potential *vs.* a copper wire acting as a pseudo reference electrode with the  $\text{Cu}^{2+}$  ions in solution ; SPR angle shift (channel 1 and 2 are separated by about 2 mm) ; and surface acoustic wave phase monitored at a fixed frequency (123.200 MHz) and converted to a frequency shift thanks to the linear phase to frequency relationship (data not shown).

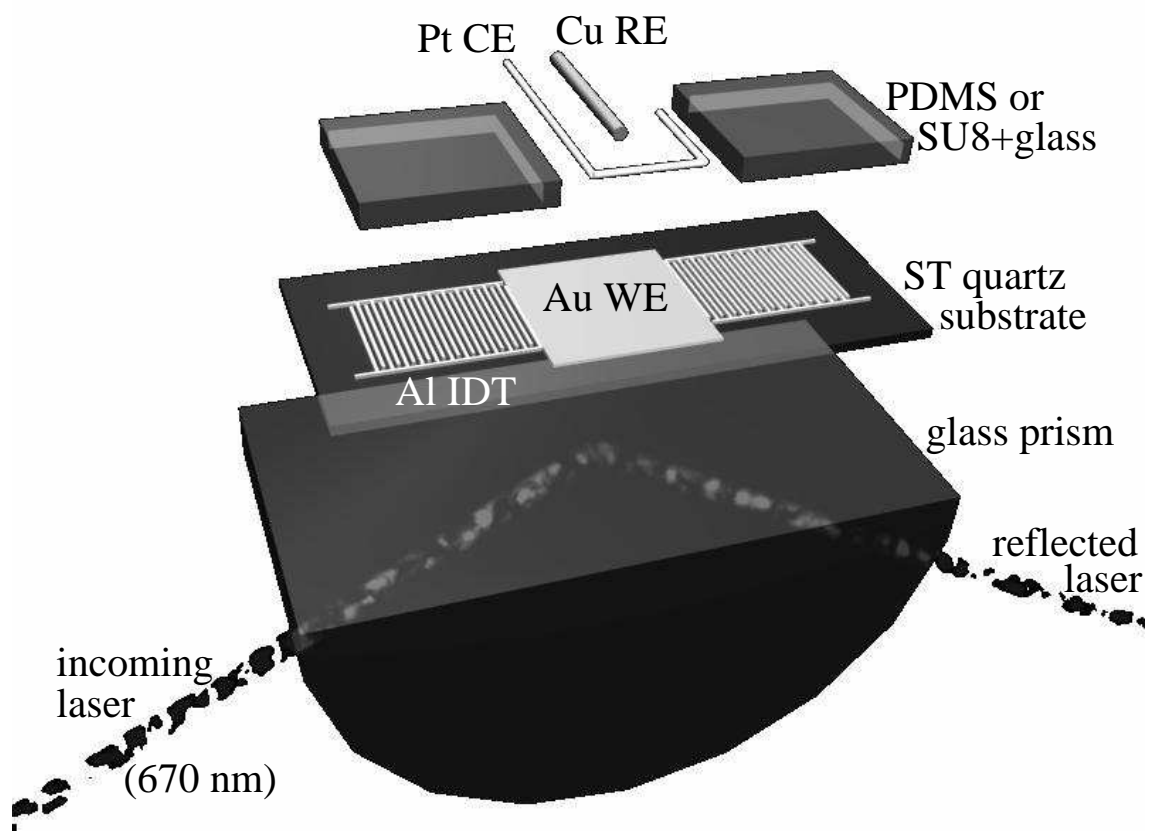
FIG. 3: Simultaneous measurement of the SAW phase at 123.200 MHz and the SPR angle shift during similar experiments: injection of buffer solution, injection of S-layer protein ( $100 \mu\text{g/ml}$ ), injection of buffer and removal of the proteins by injecting 2%  $\text{NaOCl}$ .

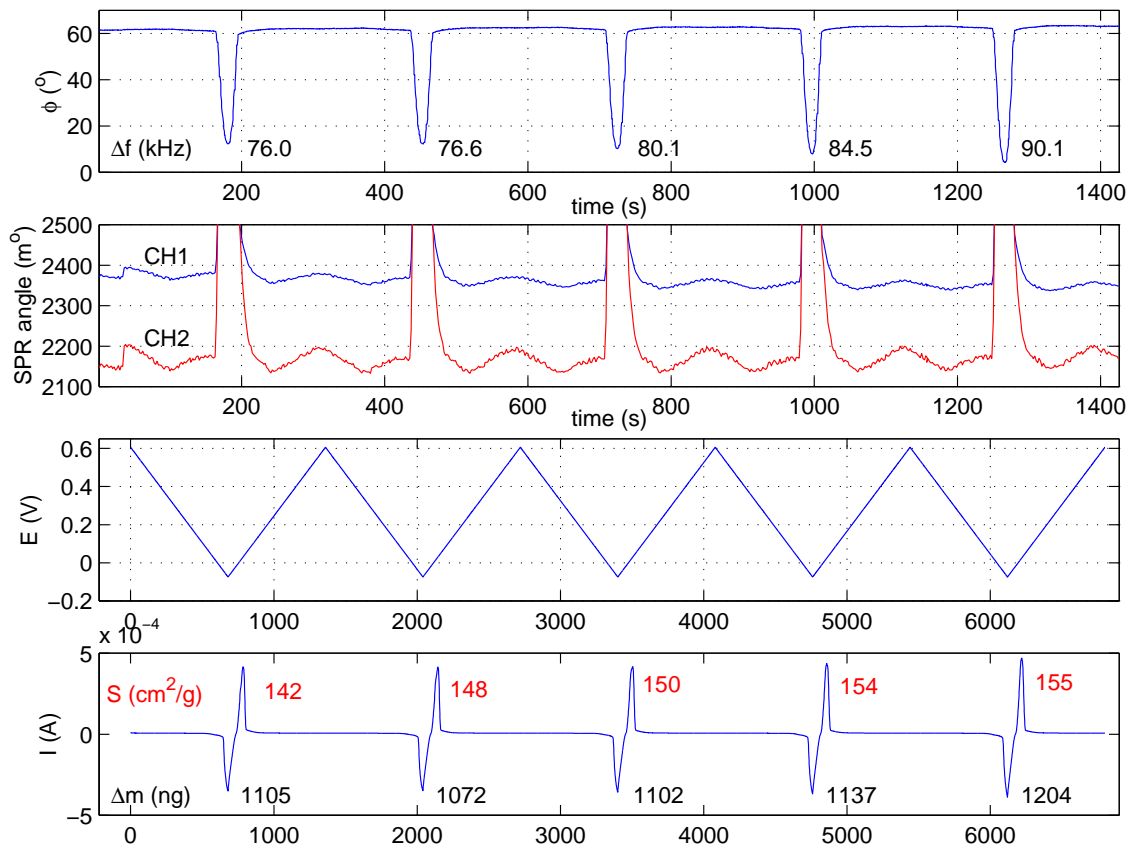
FIG. 4: Left: simulation of the SAW frequency shift for varying protein layer thickness (abscissa) and proportion of proteins in the layer (from  $x = 10\%$  to  $x = 100\%$  from right to left), and varying the density of the protein layer within the values found in the literature (from  $1.2 \text{ g/cm}^3$  as solid lines to  $1.4 \text{ g/cm}^3$  as dots). Right: simulation of the SPR angle shift for varying protein layer thickness (abscissa) and proportion of proteins in the layer (from  $x = 10\%$  to  $x = 100\%$  from bottom to top), and varying the optical index of the protein layer within the values found in the literature (from 1.45 as solid lines to 1.465 as dots). The mass density of the points lying in the region of experimentally observed angle shift have been indicated for added clarity.

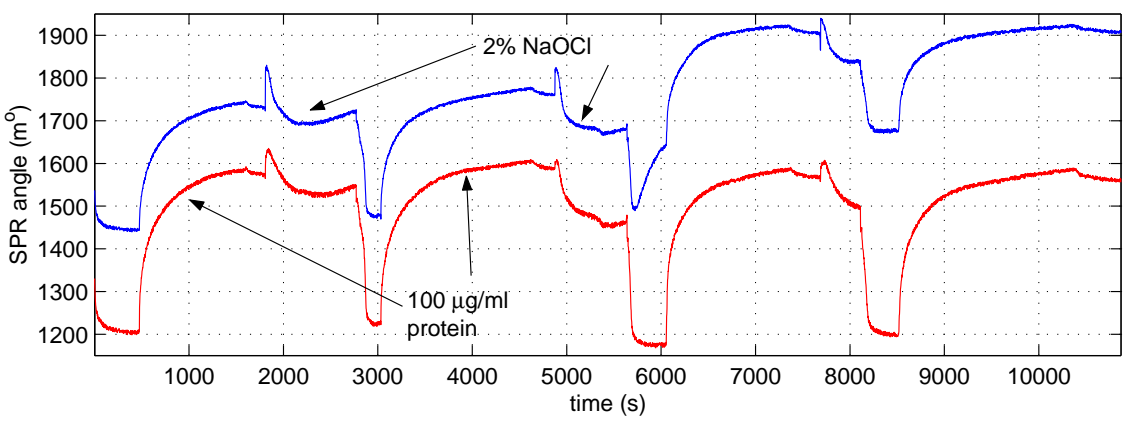
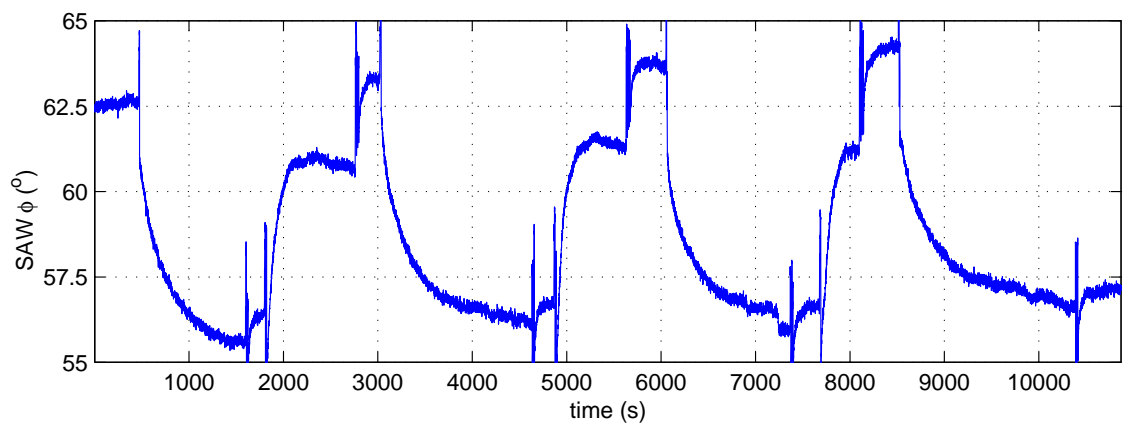
- 
- [1] B. Liedberg, C. Nylander, and I. Lundström, *Sensors and Actuators* **4**, 299 (1983)
- [2] B. Ivarsson, M. Malmqvist, *Surface plasmon resonance: development and use of BIACORE instruments for biomolecular interaction analysis*, in *Biomolecular Sensors*, Ed. E. Gizeli and C.R. Lowe (Taylor & Francis, London) 2002
- [3] F. Höök, B. Kasemo, T. Nylander, C. Fant, K. Sott, and H. Elwing, *Anal. Chem.* **73** 5796 (2001)
- [4] E. Gizeli, *Acoustic transducers*, in *Biomolecular Sensors*, Ed. E. Gizeli and C.R. Lowe (Taylor & Francis, London) 2002
- [5] M. Rodahl, P. Dahlqvist, F. Höök, B. Kasemo, *The quartz crystal microbalance with dissipation monitoring*, in *Biomolecular Sensors*, Ed. E. Gizeli and C.R. Lowe (Taylor & Francis, London) 2002
- [6] L.E. Bailey, D. Kambhampati, K.K. Kanazawa, W. Knoll, and C.W. Franck, *Langmuir* **18** 479 (2002)
- [7] A. Laschitsch, B. Menges, and D. Johansmann, *Appl. Phys. Lett.* **77** 2252 (2000)
- [8] J.-M. Friedt, L. Francis, K.-H. Choi, and A. Campitelli, *J. Vac. Sci. Technol. A* (to be published)
- [9] R. Kötz, D.M. Kolb, and J.K. Sass, *Surf. Sci.* **64** 96 (1977)
- [10] T.W. Ebbesen, H.J. Lezec, H.F. Ghaemi, T. Thio, and P.A. Wolff, *Nature* **391** 667 (1998)
- [11] A.J. Haes, and R.P. Van Duyne, *J. Am. Chem. Soc.* **124** 10596 (2002)
- [12] M. Sára, and U.B. Sleytr, *Micron* **27** 141-156 (1996)
- [13] E.S. Györvary, A. O'Riordan, A.J. Quinn, G. Redmon, D. Pum, and U.B. Sleytr, *NanoLetters* **3** 315 (2003)
- [14] B.P. Nelson, A.G. Frutos, J.M. Brockman, and R.M. Corn, *Anal. Chem.* **71** 3928 (1999)
- [15] F. Caruso, D.N. Furlong, K. Ariga, I. Ichinose, and T. Kunitake, *Langmuir* **14** 4559 (1998)
- [16] F. Höök, J. Vörös, M. Rodahl, R. Kurrat, P. Böni, J.J. Ramsden, M. Textor, N.D. Spencer, P. Tengvall, J. Gold, and B. Kasemo, *Colloids and Surfaces B* **24** 155 (2002)
- [17] R.J. Marsch, R.A.L. Jones, and M. Sferrazza, *Adsorption and displacement of a globular protein on hydrophilic and hydrophobic surfaces* *Colloids and Surfaces B* **23** 31 (2002)
- [18] E. Palik, *Handbook of optical constants of solids*, Academic Press (1997)

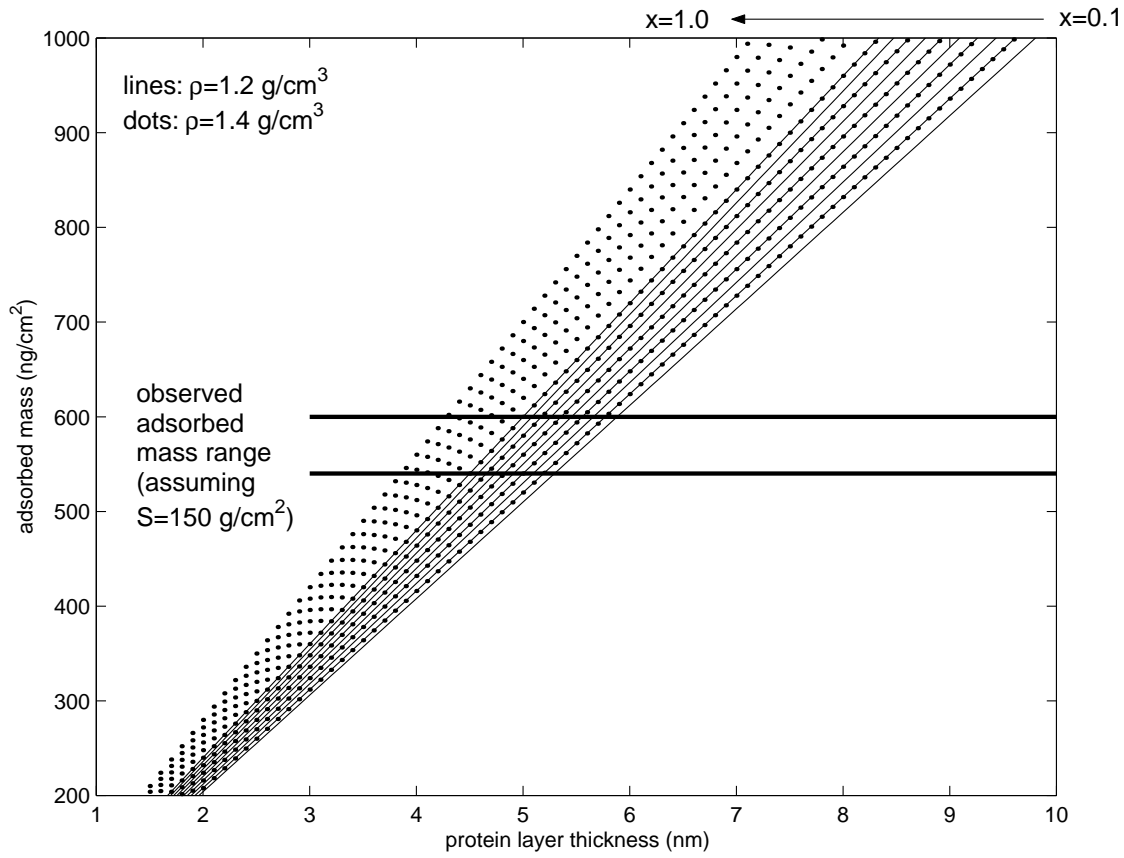


- [19] E. Stenberg, B. Persson, H. Roos, and C. Urbaniczky, *Journal of colloid and interface science* **143** 513 (1991)
- [20] M. Weygand, B. Wetzler, D. Pum, U.B. Sleytr, N. Cuvillier, K. Kjaer, P.B. Howes and M. Lösche, *Biophys. J.* **76** 458 (1999)
- [21] M. Weygand, M. Schalke, P.B. Howes, K. Kjaer, J. Friedmann, B. Wetzler, D. Pum, U.B. Sleytr, and M. Lösche, *J. Mater. Chem.* **10** 141 (2000)









glass (1.518)–1200 nm SiO<sub>2</sub> (1.45)–2 nm Ti– 55 nm Au–(protein)–water (1.33)

